"2D Symmetrical structures welding analysis obtained by FEM"

Hernández Arriaga Isaac,[a,b], Aguilera Gómez Eduardo[c], Pérez Meneses Joaquín[a]

[a]*Instituto Tecnológico de Querétaro, Av. Tecnológico S/N Esquina Gral. M. Escobedo, 76000, Querétaro,Qro., México.*
[b]*CIATEQ A.C. Centro de Tecnología Avanzada, Av. del Retablo 150, Col. Constituyentes Fovissste, 76150, Querétaro, Qro., México.*
[c]*Universidad de Guanajuato, Campus Irapuato-Salamanca, Carretera Salamanca-Valle de Santiago, 36885, Salamanca, Gto., México.*
*****Autor contacto. Dirección de correo electrónico: isaac.hernandez@ciateq.mx*

RESUMEN

En este trabajo, se lleva a cabo un estudio de los efectos de la secuencia de soldadura sobre los esfuerzos residuales y la distorsión en un marco plano simétrico reforzado. Las secuencias de soldadura apropiadas fueron determinadas utilizando reglas empíricas, ejes de simetría y centro de gravedad del marco plano, así como del concepto de círculos concéntricos. Para llevar a cabo el análisis de la secuencia de soladura se utilizó el método de elemento finito a través de un modelo termo-mecánico secuencialmente acoplado. Finalmente, se presenta un procedimiento para determinar las secuencias de soladuras apropiadas para reducir los esfuerzos residuales, la distorsión o una relación entre ambos parámetros para estructuras simétricas bidimensionales.

ABSTRACT

In this investigation, a study of the effects of the welding sequence on residual stresses and distortion in a stiffened symmetrical flat frame is developed. These proper welding sequences are obtained from empirical welding rules, axis of symmetry, center of gravity of the frame, and concentric circles. The different welding sequences are analyzed with a sequentially-coupled thermo-mechanical analysis by finite element method. Finally, this investigation presents a procedure to determine the proper welding sequences to reduce residual stress, distortion or the relation between both parameters for 2-dimensional symmetrical structures.

Keyworks: Welding sequence, residual stress, distortion, FEM.

1. Introduction

During the heating and cooling cycle in the welding process, thermal strain occurs in the filler material and in the base metal regions close to the weld. The strain produced during heating is accompanied by plastic deformation. The non-uniform plastic deformation that occurs in the welded structure is what leads to residual stresses. These residual stresses react to produce internal forces which must be equilibrated and cause distortion [1].

The residual stress and distortion in weldments depend on several interrelated factors such as thermal cycle, material properties, structural restraints, welding conditions and geometry [2]. Of these parameters, the thermal cycle has the greatest influence on the thermal loads in the welded structures. At the same time, the temperature distribution is a function of parameters such as welding sequence, welding speed, energy of the source, and environmental conditions.

A high level of tensile residual stresses near of the weld bead can induce brittle fracture, cracking due to corrosion stress, and reduced fatigue strength. Compressive residual stresses in the base metal located some distance away from the weld line can substantially decrease the critical buckling stress [3]. The main effects of distortion are the loss of tolerance in the welded components and deformation of structural elements that results in inadequate support to transfer applied loads [4]. Therefore, residual stresses and distortion should be reduced to meet all geometry and strength requirements.

Some of the most popular methods for reducing residual stresses and distortion in weld fabrication are: welding sequence [5-14], definition of welding parameters [15-17], definition of weld procedure [18], use of precambering, fixtures and prebending [19-22], thermal tensioning [23-25], heat sink welding [26], preheating [27,28], post-weld treatment [29-31], and post-weld corrective methods [32-35].

The control methods previously mentioned can increase the production costs due to energy consumption, time, and/or expensive equipment. Other methods slow down production by requiring fixture devices. Welding sequence is inexpensive because it directly affects the temperature field of the welded structure, and consequently the residual stresses and distortion. Therefore, sequence analysis is fundamental for controlling residual stresses and distortion in welded structures.

1.1. Welding sequence background

Teng and Peng [5] investigated the reduction in residual stresses caused by welding by analyzing the effects of welding sequence on residual stress distribution in single and multi-pass butt-welded plates and circular patch welds. The research was conducted through finite element-based

thermo elastic plastic analysis and simulated weld thermal cycles. Ji and Fang [6] investigated the influence of welding sequence on the residual stresses of a thick plate. Authors worked with double V-groove multiple-pass butt-welds and adopted the converse welding method between adjacent layers, or between adjacent weld beads in every layer (the converse welding method consists of applying the opposite direction between adjacent layers in multi-layer weld, or between beads in every layer). They analyzed a coupled thermo-mechanical model using finite element and an ellipsoidal heat source. The numerical results were validated against experimental results (the x-ray method). Nami, Kadivar and Jafarpur [7] investigated the effects of the welding sequence on the thermal and mechanical response of the thick plate weldments using a 3-D thermo-viscoplastic model. Anand´s viscoplastic model was used to simulate the rate dependent plastic deformation of welded materials. Also, they considered the temperature dependence of thermal and mechanical properties of material, welding speed, welding lag, and the effect of the filling material added to the weld. The model was compared with the results of two analytical and experimental works.

Mochizuki and Hayashi [8] investigated the residual stress in large-diameter, multi-pass, butt-welded pipe joints for various welding sequences. The pipe joints had an X-shaped groove. The mechanism that produces residual stress in the welded pipe joints was studied in detail using a simple prediction model. The authors worked with a thermo-elastic-plastic analysis using finite element method with an axisymmetric model. Also, they determined an optimum welding sequence for preventing stress-corrosion cracking from the residual stress distribution. Mochizuki, Hattori and Nakakado [9] studied the effect of residual stress on fatigue strength at a weld toe in a multi-pass fillet weld joint. The residual stress in the specimen was varied by controlling the welding sequence. They calculated the residual stresses by thermo-elastic-plastic analysis and compared them to strain gage and X-ray diffraction measurements. Tsai and Park [10] studied the distortion mechanisms and the effect of the welding sequence on panel distortion. In this study, distortion behaviors, including local plate bending and buckling, as well as global girder bending, were investigated using finite element analysis. It was found that buckling does not occur in structures with a skin-plate thickness of more than 1.6 mm, unless the stiffening girder bends excessively. They applied the joint rigidity method (JRM) to determine the optimum welding sequence for minimum panel warping. The JRM consists of starting with more rigid joints and progressively moving toward less rigid joints [10].

Hackmair and Werner [11] investigated the welding sequence and its effect on distortion in a T-joint structure. The T-joint structure is formed by two hollow extrusions of a 6060 T6 aluminum alloy. The extrusions are joined by four weld operations, whose order of application defines the two different welding sequences. Bart, Deepak and Kyoung [12] investigated the effect of the welding sequence on a sub-assembly composed of thin-walled aluminum alloy extruded beams. The main factor considered was the quality of the assembly after welding, which was measured by the deformation at pre-defined critical locations. The aluminum alloy extruded beam structure was modeled with a 2-D beam element model. Their methodology consisted of applying pre-estimated angular shrinkages for each welding step, thus eliminating the use of a complex nonlinear transient analysis, which would require consideration of thermo-mechanical interactions and plasticity. Two distortion modes (angular shrinkage and tilting shrinkage) were investigated and applied to welding distortion model.

Kadivar, Jafarpur and Baradaran [13] utilized a genetic algorithm method with a thermo-mechanical model to determine an optimum welding sequence. The thermo-mechanical model developed for this purpose predicts the residual stress and distortion in thin plates. The thermal history of the plate was computed with a transient, two dimensional finite element model which serves as an input to the mechanical analysis. The mechanical response of the plate was estimated through a thermo-elastic, viscoplastic finite element model. The proposed model was verified by comparison with available experimental data. The authors observed that the welding sequence changes the distribution of residual stress, but has little influence on the maximum residual stress levels. However, the welding sequence does have an effect on the weldment distortion. Therefore, the authors chose the minimization of distortion as the target function. Voutchkov, Keane, Bhaskar and Olsen [14] proposed a surrogate model that substantially reduces the computational expense in sequential combinatorial finite element problems. The model was applied to a weld path planning problem in a tail bearing housing (TBH). The TBH is a crucial component of most gas turbines and is used to help mount the engine to the body of the aircraft. The welding sequence used to attach the vanes to the inner ring was chosen to minimize distortion during the welding process.

2. Finite element model

The proposed sequentially-coupled thermo-mechanical analysis involves two steps: a transient heat transfer analysis is performed followed by a thermal elastic plastic analysis.

2.1. Thermal model

The governing equation of the heat flow follows the first law of thermodynamics (conservation of energy). This law states that the rate of change of internal energy $\rho c \dot{T}$ and conduction $\nabla \cdot q$ must be in equilibrium with the heat production Q and the power of elastic and viscoplastic straining $\dot{\varepsilon}^e$ and d^{vp}, respectively [36]:

$$\rho c \frac{\partial T}{\partial t} + \nabla \cdot \mathbf{q} = Q - \frac{E \alpha T}{1-2\nu} \dot{\varepsilon}^e + \xi s d^{vp} \quad (1)$$

The parameter ξ takes on the value of 1 if all inelastic dissipation sd^{vp} is converted into heat. The mechanical coupling terms in (1) are in most cases not considered because their influence on the temperature field is very small [37]. It is therefore possible to divide the thermo-mechanical analysis of a welding process into two main parts: the

analysis of the temperature field and subsequent analysis of the mechanical fields.

Neglecting the mechanical coupling terms in Eq. (1), the energy equation becomes [37]:

$$\rho C \frac{\partial T}{\partial t} + \nabla \cdot q = Q \tag{2}$$

Equations (1) and (2) are statements of the First Law of Thermodynamics [38]. Fourier's law of heat transfer defines a relationship between the heat flux q and the gradient of the temperature field ∇T. For an isotropic material this relationship is the Fourier heat conduction law:

$$q = -k\nabla T \tag{3}$$

Where k is the thermal conductivity for the material. Equation (2) and (3) give

$$\rho C \frac{\partial T}{\partial t} = \nabla \cdot (k \nabla T) + Q = (\{L\}^T [D] \{L\} T) + Q \tag{4}$$

In Cartesian coordinates x, y, z, equation (4) becomes

$$\left[\frac{\partial}{\partial x}\left(k_x \frac{\partial T}{\partial x}\right) + \frac{\partial}{\partial y}\left(k_y \frac{\partial T}{\partial y}\right) + \frac{\partial}{\partial z}\left(k_z \frac{\partial T}{\partial z}\right)\right] + Q(x, y, z, t)$$

$$= \rho C \, \partial T(x, y, z, t)/\partial t \tag{5}$$

Where k_x, k_y, k_z is the thermal conductivity in the x, y and z directions, respectively, $T(x, y, z, t)$ is the temperature, ρ is the density, C is the specific heat and t is time. Equation (5) becomes nonlinear if material properties k_x, k_y, k_z, ρ, and C are a function of temperature. The first term is conduction of heat through the material. The second term $Q(x, y, z, t)$ is the source of heat generation. The last term is the rate of change of internal energy.

2.2. Mechanical model

In the mechanical analysis, the temperature history obtained from the thermal analysis is introduced as a thermal loading. Thermal strains and stresses can be calculated at each time increment, and the final state of residual stresses will be accumulated by thermal strains and stresses. Residual stresses in each temperature increment are added to those at nodal points to update the behavior of the model before the next temperature increment.

Three basic sets of equation relating to the mechanical model, the equilibrium and compatibility equations and the constitutive equations for thermal elastic plastic material, are considered as follows [1]:

$$\sigma_{ij,j} + f_i = 0 \tag{6}$$

Where f_i is the sum of the body force and σ_{ij} is the Cauchy stress tensor. To ensure that the body remains continuous during the deformation, the compatibility equations must be satisfied [2]:

$$\varepsilon_{ij,kl} + \varepsilon_{kl,ij} - \varepsilon_{ik,jl} - \varepsilon_{jl,ik} = 0 \tag{7}$$

The thermal elastic plastic material model will be derived assuming isotropic material, Von Misses yield criterion and the associated flow rule and linear isotropic hardening. Thermal and mechanical properties of the selected material are a function of temperature. The micro-structural evolution is not considered. The initial assumption is that the total strain increment can be decomposed as (valid for small strains and rotations) [1]:

$$d\varepsilon_{ij} = d\varepsilon_{ij}^e + d\varepsilon_{ij}^p + d\varepsilon_{ij}^\theta \tag{8}$$

The thermo-mechanical analysis involves two steps. First, a transient heat transfer analysis is performed. The calculated transient temperatures are applied as a step-by-step thermal load. In the second step, a thermal elastic plastic analysis (quasi-static) computes the cumulative thermal stresses for each time step. The end result is residual stress and distortion.

PLANE55 and SOLID70 elements are selected for two and three dimensional thermal analysis, respectively. Both elements have a single degree of freedom, temperature and isotropic material properties [39]. PLANE42 and SOLID45 elements are selected for two and three dimensional structural analysis, respectively. PLANE 42 and SOLID45 elements have two and three degrees of freedom at each node, respectively: translation in the nodal directions and isotropic material properties [39].

Temperatures vary widely within the welded part. Therefore, thermal and mechanical properties of welded materials vary significantly [40]. The thermal and mechanical properties of ASTM A36 due to temperature are shown in Fig. 1. Autogeneous weldment was assumed. These means that weld metal, heat affected zone (HAZ), and base metal share the same thermal and mechanical properties [40].

The heat loading is simulated via weld thermal cycle curves shown in Fig. 2. The input heat is applied to all surfaces between the weld metal and the base metal.

3. Welding sequence analysis in a stiffened symmetrical flat frame

A study of the effects of the welding sequence on residual stresses and distortion in a stiffened symmetrical flat frame will be developed. The proper welding sequences obtained in this analysis are chosen to reduce residual stresses, distortion, or the relation between them. These proper welding sequences are obtained with the help of empirical welding rules, the axis of symmetry, the center of gravity of the frame, and concentric circle. The origin of the circles coincides with the center of gravity of the flat frame, and the radius of the circles is formed by the center of gravity of the flat frame with the center of gravity of each of the weld beads.

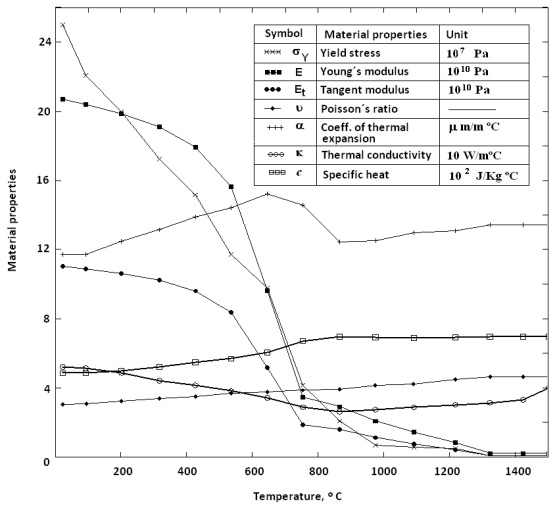

Figure 1. Thermal and mechanical properties of ASTM A36 as a function of temperature [40].

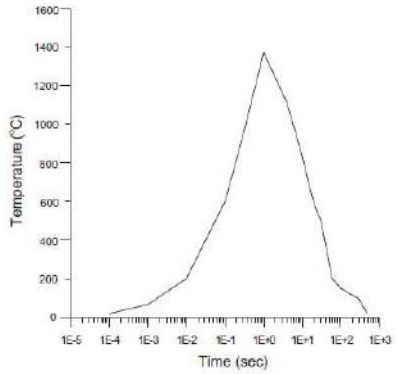

Figure 2. Weld thermal cycle of ASTM A36 carbon steel [40].

3.1. Geometric configuration of a stiffened symmetrical flat frame

The proposed symmetrical flat structure has the shape of a stiffened frame consisting of four external bars and three internal bars joined by ten weld beads (Fig. 3). This configuration is selected due to its multiple symmetries. The numbering of the weld beads is random.

3.2. Welding configuration in the stiffened symmetrical flat frame

The number of possible welding sequences depends on the number of weld beads [14]:

$$\textbf{Number of possible welding sequences} = \textbf{Number of weld beads}! \quad (9)$$

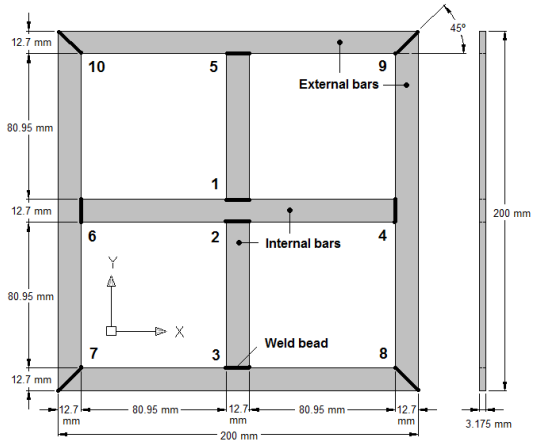

Figure 3. Geometric configuration of the stiffened symmetrical flat frame.

Applying equation (9), the number of possible welding sequences for the frame in Fig. 3 is 10! = 3,628,800. A possible approach is to run all possible combinations and select the sequence that produces the lowest distortion, the lowest residual stress or an appropriate relation between them. This is not feasible work due to the large number of possible combinations. Symmetry reduces the number of welding sequences to 1,088,640 – Still impossibly large for analysis of all options. We therefore consider empirical rules: applying the weld beads from the inside to the outside of the structure produces 9 sequences; and applying weld beads from the outside to the inside of the structure produces 9 more sequences. Therefore, only eighteen welding sequences need to be considered.

In these welding sequences, the weld beads are split in 3 groups according to their relative position to the center of gravity. A sequence is specified by the bead order 1, 2,..9 and the letters I-O (starting from the inside) or O-I (starting from the outside). The term WT means that welding tacks are used to keep the structure fixed while performing the welding process. Experience shows that the welding tacks (WT), together with the welding sequence, have important effects on residual stresses and distortion in the welded structures. Therefore, each of the 18 welding sequences will be considered with and without welding tacks, for a total of 36 numerical simulations –a tractable problem. The configurations of these welding sequences are shown in Table 1.

3.3. Finite element model of the stiffened symmetrical flat frame

The numerical simulations of the different welding sequences are based on the numerical model of the welding process developed in the I-type structure subject to tension, considering the time between the application of a weld bead and the next. To simulate the structure with welding tacks,

the elements of the welded region are activated during all the analysis. To simulate the structure without welding tacks, the elements of the welded region are first deactivated and then activated in accordance with the welding sequence. Thermal and mechanical properties are deactivated by means of a reduction factor (1e-6). The welding region has a fine mesh and the zones away from the weld bead are meshed coarser. This consideration reduces the processing time and still guarantees computational accuracy. Fig. 4 shows the finite element model of the stiffened symmetrical flat frame.

Table 1. Welding sequences used in the stiffened symmetrical flat frame.

Welding sequence	Configuration
1 I-O	1-2-3-4-5-6-7-8-9-10
2 I-O	1-2-5-3-4-6-8-7-10-9
3 I-O	1-2-3-6-4-5-7-8-9-10
4 I-O	1-2-3-4-5-6-7-9-8-10
5 I-O	1-2-5-3-4-6-8-10-7-9
6 I-O	1-2-3-4-6-5-9-7-8-10
7 I-O	1-2-3-4-5-6-7-10-8-9
8 I-O	1-2-5-3-4-6-8-7-9-10
9 I-O	1-2-3-6-4-5-7-10-8-9
1 O-I	10-9-8-7-6-5-4-3-2-1
2 O-I	9-10-7-8-6-4-3-5-2-1
3 O-I	10-9-8-7-5-4-6-3-2-1
4 O-I	10-8-9-7-6-5-4-3-2-1
5 O-I	9-7-10-8-6-4-3-5-2-1
6 O-I	10-8-7-9-5-6-4-3-2-1
7 O-I	9-8-10-7-6-5-4-3-2-1
8 O-I	10-9-7-8-6-4-3-5-2-1
9 O-I	9-8-10-7-5-4-6-3-2-1

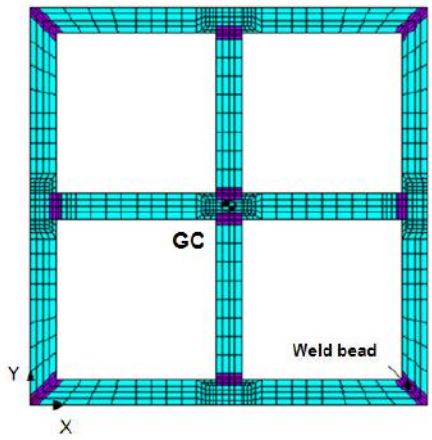

Figure 4. Finite element model of the stiffened symmetrical flat frame.

Thermal initial and boundary conditions

(a) Initial condition
Because the thermal model consists of a transient heat transfer analysis, it is required an initial condition of the base metal, which is considered as the surrounding temperature (T_0=20°C).

(b) Boundary conditions (see Fig. 4)
Surfaces in contact with the surrounding except surfaces belonging to the weld beads (Plane x-y in z=0):

$$\boldsymbol{\kappa}\frac{\partial \mathbf{T}}{\partial \mathbf{n}}(\mathbf{x},\mathbf{y},\mathbf{z},\mathbf{t}) = -\mathbf{h_c}[\mathbf{T}_\infty - \mathbf{T_s}] \quad (10)$$

Nodes belonging to weld beads (according to the welding sequence):

$$\boldsymbol{\kappa}\frac{\partial \mathbf{T}}{\partial \mathbf{n}}(\mathbf{x},\mathbf{y},\mathbf{z},\mathbf{t}) = \mathbf{q_s} \quad (11)$$

Prescribed heat input: heat loading is simulated via weld thermal cycle curves (Fig. 2). Heat is applied on all surfaces between the weld metal and the base metal according to welding sequence.

Mechanical boundary conditions

Three boundary conditions are applied to structural model (see Fig. 4).

(a) The nodes belonging to the element attached to its center of gravity of the structure are selected to prevent rigid body motion and rigid body rotations:

$$\mathrm{u} = \mathrm{v} = 0;\ \varepsilon_x = \frac{\partial u}{\partial x} = 0;\ \varepsilon_y = \frac{\partial v}{\partial y} = 0 \quad \text{and}$$

$$\omega_z = \frac{1}{2}\left(\frac{\partial \mathrm{v}}{\partial \mathrm{x}} - \frac{\partial \mathrm{u}}{\partial \mathrm{y}}\right) = 0 \quad (12)$$

(b) Plane-stress problem: The normal stresses to the plane X-Y (σ_z) and shearing stress acting in this plane (τ_{xz} and τ_{yz}) are zero on face of the structure. Therefore; $\sigma_x = \sigma_y = \tau_{yx} \neq 0$.

(c) Surfaces in contact with the surrounding: The normal stresses to the surfaces in contact with the surrounding and the shear stresses are zero (i.e., in x=0, $\sigma_x = \tau_{yz} = 0$).

Solution of the finite element model of the stiffened symmetrical flat frame

After completing the finite element mesh and specifying the loading conditions (initial and boundary conditions and body loads), the solution can be initiated. In the transient thermal analysis, the time to complete each weld bead is 6 seconds. Thermal elastic plastic analysis for each simulation requires 33 load steps to complete the weld thermal cycles.

4. Analysis and Results of residual stress-distortion relation

The following equation is proposed for quantitative comparison of the effects of the welding sequence on residual stress, distortion, or the relation between them:

$$\mathrm{R(RS\ vs\ DISTORTION)} = \mathbf{W}\left(\frac{\sigma_{current}}{\sigma_{max(U_{min})}}\right) + \mathbf{P}\left(\frac{U_{current}}{U_{max(\sigma_{min})}}\right) \quad (13)$$

Where $\sigma_{current}$ and $U_{current}$ are the residual stress and distortion for each welding sequence. The residual stress corresponds to one selected point on the structure and the distortion corresponds to the maximum distortion that occurs in each welding sequence. The highest residual stress that occurs in all welding sequences $\sigma_{max}(U_{min})$ is accompanied by lowest distortion. The highest distortion that occurs in all welding sequences $U_{max}(\sigma_{min})$ is accompanied by lowest residual stress. Weight factors W and P can be assigned to residual stress and distortion, respectively. For the case when the welding sequence only reduces the residual stress, $W = 1$ and $P = 0$. When the welding sequence only reduces distortion, $W = 0$ and $P = 1$. When the welding sequence reduces the relation between both parameters, $W + P = 1$.

4.1. Order of importance of the welding sequences in the stiffened symmetrical flat frame

Applying equation (13) to the results of the residual stress and distortion obtained in the 36 numerical simulations, the order of importance of the different welding sequences to reduce residual stress, distortion, or a relation between them is obtained (Table 2). Analyzing these results, the proper welding sequence to reduce residual stress is 5 I-O (from the inside to the outside of the structure), and the proper welding sequence to reduce the distortion is 5 O-I WT (from the outside to the inside using welding tacks). This implies that the proper welding sequence to reduce the residual stresses is inappropriate to reduce the distortion and vice versa. Finally, welding sequence 1 I-O (welding sequence in growing spiral) shows the best overall performance: it is ranked number 4 in reducing stress and 19 in reducing distortion. Therefore, welding sequence 1 I-O is the proper welding sequence to improve the relation between the selected critical parameters.

4.2. Proper welding sequences to reduce the residual stress, distortion, or a relation between them in the stiffened symmetrical flat frame

To formulate the proper welding sequences obtained in Table 2, the axis of symmetry and the center of gravity of the flat frame are used. We draw concentric circles centered on the center of gravity of the frame and extending to the center of gravity of the weld beads. The weld beads located at the same distance from the center of gravity of the frame fall on the same circle. The circles are numbered from the smallest to the largest. Weld beads 1 and 2 belong to circle 1, weld beads 3, 4, 5, and 6 belong to circle 2, and weld beads 7, 8, 9, and 10 belong to circle 3 (Fig. 5).

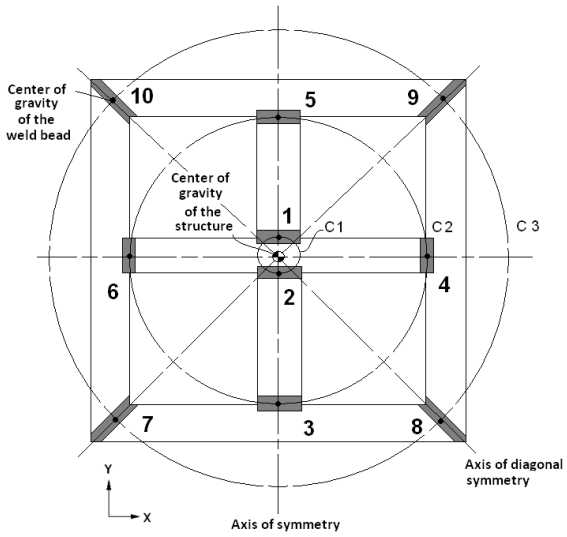

Figure 5. Centers of gravity of the structure, centers of gravity of the weld beads, axis of symmetry, and concentric circles in the stiffened symmetrical flat frame.

4.3. Proper welding sequence to reduce the residual stress in the stiffened symmetrical flat frame

This welding sequence begins by selecting the weld beads belonging to the smallest circle and then continuing with the weld beads belonging to the larger circle until the largest circle is reached. Weld beads within the same circle should be selected symmetrically. First, the weld beads with diagonal symmetry are selected. If the weld bead with diagonal symmetry has already been selected, then the farthest symmetrical weld bead is selected next. When a current weld bead has more than one farthest symmetrical weld bead (weld beads with the same radius); the adjacent weld bead in counter-clockwise is selected next. Finally, to move from one circle to the other, the farthest weld bead to the current weld bead is selected next. If a current weld bead has more than one farthest weld bead, the adjacent weld bead in counter-clockwise is selected.

4.4. Proper welding sequence to reduce distortion in the stiffened symmetrical flat frame

This welding sequence requires applying weld tacks to the structure. The sequence begins by selecting the weld beads belonging to the largest circle, and then continuing with the weld beads belonging to the adjacent smaller circle until the smallest circle is reached. The application of the weld beads belonging to the same circle should be selected in a symmetrical form. First, the weld beads with diagonal symmetry are selected. If the weld bead with diagonal symmetry has already been selected previous to the current

weld bead, then the farthest symmetrical weld bead is selected next. When a current weld bead has more than one farthest symmetrical weld bead, the adjacent weld bead in counter-clockwise is selected next. Finally, to move from one circle to the other, the farthest weld bead to the current is selected next. If a current weld bead has more than one farthest weld bead, the adjacent bead in a clockwise manner is selected.

4.5. Proper welding sequence to improve the relation between both critical parameters in the stiffened symmetrical flat frame

It is observed in Table 2 that the welding sequence 1 I-O shows the best stress-distortion relation, ranking number 4 in stress reduction and 19 in distortion reduction. Therefore, welding sequence 1 I-O is selected to improve the relation between the two parameters. This welding sequence starts with the beads in the smallest circle and then continuing with the beads in the larger adjacent circle until the largest circle is reached. Weld beads within the same circle should be applied in counter-clockwise direction. To move from one circle to the next, the closest weld bead is selected.

4.6. Procedure to determine the proper welding sequences to reduce residual stress, distortion or a relation between them in symmetrical structures in two dimensions

Based on the welding sequence analysis developed in the stiffened symmetrical flat frame, the following procedures are obtained to determine proper welding sequences in symmetrical structures in 2 dimensions. To determine the proper welding sequence to reduce the residual stress, distortion, or a relation between them in symmetrical structures in the plane, all procedures are as follows: Determine the axis of symmetry and the center of gravity of the structure. Draw concentric circles centered on the center of gravity of the structure and extending to the center of gravity of each of the weld beads. The weld beads located at the same distance from the center of gravity of the structure fall on the same circle. The circles are numbered from the smallest to the largest.

To reduce residual stress: Start with the weld bead on the smallest circle and then continue with the weld beads on the larger adjacent circle until the largest circle is reached. The weld beads on the same circle should be symmetrical. First, the weld beads with diagonal symmetry are selected. If the weld bead with diagonal symmetry has already been selected, then the farthest symmetrical weld bead is selected next. When a current weld bead has more than one farthest symmetrical weld bead, the adjacent weld bead in counter-clockwise direction is selected. Finally, to move from one circle to the other, the farthest weld bead to the current weld bead is selected. If a current weld bead has more than one farthest weld bead, the adjacent weld bead in counter-clockwise direction is selected. The converse welding method between weld beads is adopted.

To reduce Distortion: Apply welding tacks to the structure before welding. First, the weld beads in the largest circle are selected, followed by the weld beads on the adjacent smaller circle, until the smallest circle is reached. The application of the weld beads on the same circle should be in symmetrical form. The weld beads with diagonal symmetry are selected first. If the weld bead with diagonal symmetry has already been selected, then the farthest symmetrical weld bead is selected next. When a current weld bead has more than one farthest symmetrical weld bead, the adjacent weld bead in counter-clockwise direction is selected next. Finally, to move from one circle to the other, the farthest weld bead to the current is selected. If a current weld bead has more than one farthest weld bead, the adjacent weld bead in a clockwise direction is selected. The converse welding method between weld beads is adopted.

To improve the Residual Stress-Distortion relation: First, the weld beads on the smallest circle are selected and then continuing with the weld beads on the larger adjacent circle until the largest circle is reached. The application of weld beads on the same circle should be in an adjacent form in counter-clockwise direction. To move from one circle to the other, the closest weld bead to the current is selected. The converse welding method between weld beads is adopted.

5. Conclusions

Based on the results presented herein, we can conclude the following:

- The welding sequence that produces the lowest distortion also produces the highest residual stress and vice-versa.
- For the stiffened symmetrical flat frame, the distortion is reduced by 35 %, while the maximum Von Misses residual stress is reduced by 15% when applying the proper welding sequence to respectively reduce distortion or residual stress. The welding sequence is twice as effective for reducing distortion as for reducing residual stresses.
- Welding tacks are not recommended when trying to reduce residual stress.
- Welding tacks are necessary to reduce distortion.
- Welding tacks followed by weld bead application from the outside to the inside of the structure reduces distortion but increases residual stresses.
- Applying the weld beads from the inside to the outside of the structure without welding tacks reduces the residual stress but increases the distortion.

- The relation between P=0,5 and W=0,5 does not mean that both parameters are reduced by the same percentage, because the proper welding sequence reduces the distortion twice as much as residual stresses.

REFERENCES

[1] Zhili, F., 2005, "Processes and Mechanisms of Welding Residual Stress and Distortion", CRC Press

[2] Masubuchi, K., 1980, "Analysis of Welded Structures: Residual Stresses, Distortion, and their Consequences", Pergamon Press.

[3] Masubuchi, K., 2001, "Welding Handbook: Residual Stress and Distortion", American Welding Society, 9th edition.

[4] Messler, R., 1999, "Principles of Welding: Processes, Physics, Chemistry, and Metallurgy", John Wiley and Sons, Inc.

[5] Tso, L. T., Peng, H. C., Wen, C. T., 2003, "Effect of welding sequence on residual stresses", Computer and Structures, 81: 273-286.

[6] Ji, S. D., Fang, H. Y., Liu, X. S., Meng, Q. G., 2005, "Influence of a welding sequence on the welding residual stress of a thick plate", Modeling and Simulation in Materials Science and Engineering, 13: 553-565.

[7] Nami, M. R., Kadivar, M. H., Jafarpur, K., 2004, "3D thermo-viscoplastic modeling of welds: Effect of piece-wise welding on thermo-mechanical response of thick plate weldments", Iranian Journal of Science and Technology, Transaction B, Vol. 28, No. B4, 467-478

[8] Mochizuki, M., Hayashi, M., 2000, "Residual stress distribution depending on welding sequence in multi-pass welded joints with X-shaped groove", ASME J. Pressure Vessel Technology. 122: 27-32.

[9] Mochizuki, M., Hattori, T., Nakakado, K., 2000, "Residual stress reduction and fatigue strength improvement by controlling welding pass sequence", ASME J. Engineering Materials and Technology, 122: 108-112.

[10] Tsai, C. L., Park, S. C., Cheng, W. T., 1999, "Welding distortion of a thin-plate panel structure", Weld. J. 78 (11): 156s-165s.

[11] Hackmair, C., Werner, E., Pönisch, M., 2003, "Application of welding simulation for chassis components within the development of manufacturing methods", Computational materials Science, 28: 540-547.

[12] Bart, O. N., Deepak, G., Kyoung, Y. K., 2004, "Welding distortion minimization for an aluminum alloy extruded beam structure using a 2D model", ASME J. Manufacturing Science and Engineering, 126: 52-63.

[13] Kadivar, M. H., Jafarpur, K., Baradaran, G. H., 2000, "Optimizing welding sequence with genetic algorithm", Computational Mechanics. 26: 514-519.

[14] Voutchkov, I., Keane, A. J., Bhaskar, A., Olsen, T. M., 2005, "Weld sequence optimization: the use of surrogate models for solving sequential combinatorial problems", Computer methods in applied mechanics and engineering, 194: 3535-3551

[15] Murugan, V., Gunaraj, V., 2005, "Effects of Process parameters on angular distortion of gas metal arc welded structural steel plates", Weld. J. 84 (11): 165s-171s.

[16] Tso-Liang Teng., Ching-Cheng Lin., 1998, "Effect of welding condition on residual stress due to butt welds", Int. J. Pressure Vessels and Piping, 75: 857-864.

[17] Siddique M., Abid M., Junejo H. F., Mufti A., 2005, "3-D Finite element simulation of welding residual stresses in pipe-flange joints: effects of welding parameters", Materials Science Forum, Vols. 490-491, pp 79-84.

[18] Bhide, S. R., Michaleris, P., Posada, M., Deloach, J., 2006, "Comparison of buckling distortion propensity for SAW, GMAW, y FSW", Weld. J. 85 (9): 189s-195s.

[19] Jang, B., Kim, H. K., Kang S., 2001, "Effects of root opening on mechanical properties, deformation and residual stress of weldments", Weld. J. 80 (7): 80s-88s.

[20] Wahab, M. A., Alam, M. S., Painter, M. J., Stafford, P. E., 2006, "Experimental and numerical simulation of restraining forces in gas metal arc welded joints", Weld. J. 85 (2): 35s-43s.

[21] Muhammad, Abid., Muhammad, Siddique., 2005, "Numerical simulation of the effect of constraints on welding deformations and residual stresses in a pipe-flange joint", Modeling Simul. Mater. Sci. Eng. 13: 919-933.

[22] Cheng C.M., 2007, "Butt-welding residual stress of heat treatable aluminum alloys" J. Mater. Sci. Technol., Vol.23, No.2: 217-222.

[23] Michaleris, P., Sun, X., 1997, "Finite Element Analysis of Thermal Tensioning Techniques Mitigating Weld Buckling Distortion", Weld. J. 76(11): 451s-457s.

[24] Michaleris, P., Dantzig, J., Tortorelli, D., 1999, "Minimization of welding residual stress and distortion in large structures", Weld. J. 78 (11): 361-366.

[25] Shaoqing G., Xiaohong L., 2000, "Welding Distortion Control of thin Al alloy plate by static thermal tensioning", J. Mater. Sci. Technol, Vol.17, No. 1: 163-164.

[26] Engelhard G., Habip L. M., Pellkofer D., Schmidt J., Weber J., 2000, "Optimization of residual welding stresses in austenitic steel piping: prooftesting and numerical simulation of welding and postwelding processes", Nuclear Engineering and Design, Vol. 198: 141-151.

[27] Lin Y. C., Lee K. H., 1997,"Effect of preheating on the residual stress in type 304 stainless steel weldments", Journal of Materials Processing Technology, Vol. 63: 797-801.

[28] Adedayo S. M., Adeyemi M. B., 2000, "Effects of Preheat on residual stress distributions in arc-welded mild steel plates", ASM International. Journal of Materials Engineering and Performance, Vol. 9 (1): 7-11.

[29] Cho J. R., Lee B. Y., Moon Y. H., Van Tyne C. J., 2004, "Investigation of residual stress and post weld heat treatment of multi-pass welds by finite element method and experiments", Journal of Materials Processing Technology, 155-156: 1690-1695.

[30] Cheng X., Fisher J. W., Prask H. J., Gnäupel-Herold T., Yen B. T., Roy S., 2003, "Residual stress modification by post-weld treatment and its beneficial effect on fatigue strength of welded structures", International Journal of Fatigue, Vol. 25:1259-1269.

[31]Olabi, A. G., Hashmi M. S. J., 1998, "Effects of the stress-relief conditions on a martensite stainless-steel welded component", Journal of Materials Processing Technology, Vol. 77: 216-225.

[32] Aoki, S., Nishimura T., Hiroi T., Hirai S., 2007, "Reduction method for residual stress of welded joint using harmonic vibrational load", Nuclear Engineering and Design, Vol. 237: 206-212

[33] Xuesong L., Hongyuan F., Shude J., and Zhibo D., 2003, "Control of titanium alloy thin plate welding distortion by trailing penning", J. Mater. Sci. Technol., Vol.19, Suppl. 1: 184-186.

[34] Quanhong L., Jing C., Huanining C., 2001,"Possibility of inducing compressive residual stress in welded joints of SS400 steels", J. Mater. Sci. Technol., Vol.17, No.6: 661-663.
[35] Zhang J., Liu K., Zhao K., Li X., Liu Y., Zhang K., 2005, "A study on the relief of residual stresses in weldments with explosive treatment", International Journal of Solids and Structures, Vol. 42:3794-3806.
[36] Karlsson, L., 1986, "Thermal Stresses I-Chapter 5: Thermal Stresses in welding", Edited by Hetnarski R. B., Elsevier Science Publishers B.V.
[37] Argyris, J. H., Szimmat, J., William, K. J., 1982, "Computational aspect of welding stress analysis", Computer methods in applied mechanics and engineering, 33: 635-666.
[38] Boley, B., Weiner, J., 1962, "Theory of thermal stresses", John Wiley and Sons, Second Edition.
[39] Swanson Analysis Systems, Inc. "III ANSYS user´s manual: Elements", Vol.
[40] Chang, P. H., 2003, "Numerical and experimental investigation on residual stresses of the butt-welded joints", Computation Material Science, 29: 511-522

Table 2. Order of importance of the analyzed welding sequences in the stiffened symmetrical flat frame

Welding sequence	Parameters		Order of importance of welding sequence to reduce:			
			Residual stress		Distortion	
	Umax (mm)	σ_{vm} Node 681(Mpa)	W=1, P=0	Ranking	W=0, P=1	Ranking
1 I-O	0.286	205.48	0.872	**4**	0.905	**19**
2 I-O	0.314	201.29	0.854	**2**	0.994	**35**
3 I-O	0.293	208.27	0.883	**12**	0.927	**25**
4 I-O	0.305	205.73	0.873	**6**	0.965	**32**
5 I-O	0.316	199.84	0.848	**1**	1	**36**
6 I-O	0.297	207.6	0.881	**10**	0.940	**28**
7 I-O	0.309	206.46	0.876	**8**	0.978	**33**
8 I-O	0.312	201.72	0.856	**3**	0.987	**34**
9 I-O	0.290	208.54	0.885	**14**	0.918	**23**
1 O-I	0.277	206.3	0.875	**7**	0.877	**17**
2 O-I	0.220	223.64	0.949	**31**	0.696	**8**
3 O-I	0.228	216.30	0.918	**30**	0.722	**10**
4 O-I	0.278	205.52	0.872	**5**	0.880	**18**
5 O-I	0.214	224.22	0.951	**33**	0.677	**3**
6 O-I	0.230	215.32	0.913	**27**	0.728	**11**
7 O-I	0.277	210.90	0.895	**18**	0.877	**16**
8 O-I	0.223	223.70	0.949	**32**	0.706	**9**
9 O-I	0.235	214.29	0.909	**24**	0.744	**12**
1 I-O WT	0.296	210.33	0.892	**15**	0.937	**26**
2 I-O WT	0.299	208.1	0.883	**13**	0.946	**30**
3 I-O WT	0.290	212.3	0.901	**23**	0.918	**22**
4 I-O WT	0.289	210.53	0.893	**16**	0.915	**21**
5 I-O WT	0.300	206.79	0.877	**9**	0.949	**31**
6 I-O WT	0.291	211.95	0.899	**22**	0.921	**24**
7 I-O WT	0.297	211.43	0.897	**20**	0.940	**27**
8 I-O WT	0.298	207.8	0.881	**11**	0.943	**29**
9 I-O WT	0.287	214.67	0.911	**26**	0.908	**20**
1 O-I WT	0.260	211.05	0.895	**19**	0.823	**14**
2 O-I WT	0.212	231.75	0.983	**35**	0.671	**2**
3 O-I WT	0.219	214.58	0.910	**25**	0.693	**7**
4 O-I WT	0.266	210.45	0.893	**17**	0.842	**15**
5 O-I WT	0.206	235.74	1	**36**	0.652	**1**
6 O-I WT	0.216	215.20	0.913	**28**	0.684	**5**
7 O-I WT	0.260	211.52	0.897	**21**	0.823	**13**
8 O-I WT	0.215	231.39	0.982	**34**	0.680	**4**
9 O-I WT	0.217	215.75	0.915	**29**	0.687	**6**

